

International Research Journal on Advanced Engineering Hub (IRJAEH)

e ISSN: 2584-2137

Vol. 03 Issue: 09 September 2025

Page No: 3819-3825

https://irjaeh.com

https://doi.org/10.47392/IRJAEH.2025.0555

Intrusion Detection System in CAN-BUS Vehicle Networks Using Machine Learning

Deekshith G. R.¹, S. R. Sheetal², Divya G. S.³, Darshan B. M.⁴, Aryan Anil⁵, Balakrishna V⁶

1,2,3,4,5,6</sup>Department of Computer Science, AMC Engineering College, Bengaluru, India

Email: deekshith.gr123@gmail.com¹, srsheeta@gmail.com², Divya.siddaraj@gmail.com³, mahadeva3008@gmail.com⁴, aryananil00007@gmail.com⁵, balureddy2004@gmail.com⁶

Abstract

As vehicles become more connected and software-rich, securing communications inside vehicles is increasingly important. The Controller Area Network (CAN-BUS) is simple and efficient, which is why it remains the dominant vehicle network. That simplicity comes at a cost: the protocol lacks built-in authentication or encryption, leaving it exposed to injection, flooding and impersonation attacks. Here we describe a practical, real-time Intrusion Detection System (IDS) for CAN-BUS that combines supervised machine learning with features useful for deployment. The core detector is a Random Forest trained on the OCS-Lab dataset; it distinguishes benign traffic from DoS, fuzzy and impersonation attacks and achieves a validation accuracy of 85.37%. Importantly, the IDS is more than a model: it includes a retraining dashboard, a timeline for investigation, live packet classification and automated email alerts so operators can react quickly and with context.

Keywords: Automotive cybersecurity; CAN-BUS; Intrusion detection system; Machine learning; Real-time monitoring.

1. Introduction

Modern vehicles host many electronic control units (ECUs) that coordinate critical functions such as engine control, brake, body electronics and driver assistance. CAN-BUS is the standard in-vehicle backbone because it provides deterministic arbitration and a degree of fault tolerance. That same simplicity, however, leaves out cryptographic protections. An attacker with local access — through OBD-II, a compromised telematics module, or an aftermarket device — can inject frames, flood the bus, or impersonate ECUs; any of these actions can degrade availability or, worse, safety.

- **Motivation:** Effective protections must run in real time on constrained hardware and give operators concise, actionable signals so they can triage incidents quickly.
- Contributions: This work presents (i) a modular ML-based IDS with operator-facing dashboards and automated alerts. (ii) an end-to-end capture-to-alert pipeline; (iii) an empirical evaluation using OCS-Lab data; and (iv) deployment guidance covering latency, observability and maintenance.

2. Background on CAN-BUS

2.1. Frame Structure and Arbitration

A standard CAN frame includes an identifier (11- or 29-bit), control fields (including DLC), up to eight data bytes, CRC, ACK and EOF. Arbitration uses wired-AND: nodes with lower identifier values win access to the bus. This scheme supports real-time priorities but can be abused — an attacker who repeatedly sends a high-priority identifier can effectively deny service.

2.2. Error Handling and Fault Confinement

CAN controllers track transmits and receives error counters; exceeding thresholds causes nodes to enter error-passive or bus-off modes and stop transmitting. Attackers can deliberately cause errors using malformed frames. Because low-level counters are not always exposed to applications, our IDS emphasizes timing and distributional statistics that a passive capture can reliably observe.

3. Related Work

The literature includes interval and frequency detectors [1], temporal deep models [2], and broader system-level analyses [4]. Recent surveys and



Vol. 03 Issue: 09 September 2025

Page No: 3819-3825

https://irjaeh.com

https://doi.org/10.47392/IRJAEH.2025.0555

comparative analyses summarize AI- driven invehicle IDS approaches and provide a taxonomy of features and learning methods; this help place our work in the context of practical, deployment-aware IDS research. Recent empirical studies show continuing improvements in sequence and distributional approaches for CAN IDS. [6]–[8]

4. Problem Formulation

We frame intrusion detection as a multi-class classification problem with labels for benign, DoS, fuzzy, and impersonation attacks. Let $D = \{(xi, yi)\}$ N be chronological, windowed samples with labels $yi \in \{0, 1, 2, 3\}$. Each feature vector $xi \in Rd$ contains message-level, temporal and distributional statistics. The learning objective is to find $f\theta: Rd \rightarrow \{0, 1, 2, 3\}$ that maximizes macro-F1 under latency constraints compatible with gateway deployment. We also incorporate calibrated scores so alerts can be tired by operator severity.

5. System Design and Methodology

Figure 1 shows the layered pipeline: capture \rightarrow preprocess \rightarrow classify \rightarrow visualize/log \rightarrow alert. A key engineering choice is to isolate inference from non-critical subsystems (storage, email), so temporary service outages do not block detection.

5.1. Dataset

We use the OCS-Lab CAN intrusion dataset [3], which includes benign traces and labeled attacks (DoS, fuzzy, impersonation). Each record contains a timestamp, identifier, DLC and up to eight payload bytes. Attack classes primarily differ in timing and payload variability.

5.2. Threat Model and Assumptions

The attacker has local access to the CAN segment (can inject, replay or flood frames). The IDS operates as a read-only gateway or passive tap. We assume legacy CAN without cryptographic protection.

5.3. Feature Engineering and Windowing

Representative features appear in Table 1: message-level encodings (ID hashing/one-hot, DLC, payload histograms), per-ID timing statistics, and short-window aggregates (unique ID ratio, top-k frequency share). Continuous features are Minmax scaled. Windows of n=50 frames with 50% overlap provide a practical compromise between responsiveness and stability.

Table 1 Representative Feature Set (abbrev.)

Table 1 Representative 1 catale Set (abble):		
Feature	Type	
ID one-hot / hashed buckets	Categorical	
DLC	Numeric	
Payload byte histogram (coarse bins)	Numeric vector	
Inter-arrival time (per ID)	Temporal numeric	
Unique-ID ratio (window)	Temporal stat	
Top-k ID frequency share	Temporal stat	

5.4. Preprocessing and Split

We filter malformed frames, compute per-ID deltas, and assemble sliding windows in chronological order. To avoid leakage, we split chronologically: 70% train, 15% validation, 15% test.

5.5. Model Selection and Hyperparameters

We evaluated Random Forest (RF), SVM (RBF) and Gradient Boosting. RF provided the best trade-off between accuracy and inference latency on gateway-class hardware. Typical RF hyperparameters used: 300 trees, max depth 18, min samples split 4, class weight=balanced, max features=sqrt.

5.6. Training and Inference Workflow

Algorithm 1 summarizes training and inference: feature ex- traction, chronological splits, class-weighted training, artifact persistence (model, scaler, feature map), and batched inference (128 windows) with post-processing and thresholding.

Table 2 Algorithm 1 Training and Inference Workflow

VV OI KIIOW
Algorithm 1 Training and Inference
Workflow
1: Load frames; compute features (Table 1);
build windows
2: Chronological split: 70/15/15 train/Val/test
3: Train RF with class weighting; tune
trees/depth on validation
4: Persist best model via job lib; export
scaler/feature map
5: Inference: vectorize \rightarrow batch predict (128)
→ post-process

IRJAEH

e ISSN: 2584-2137

Vol. 03 Issue: 09 September 2025

Page No: 3819-3825

https://irjaeh.com

https://doi.org/10.47392/IRJAEH.2025.0555

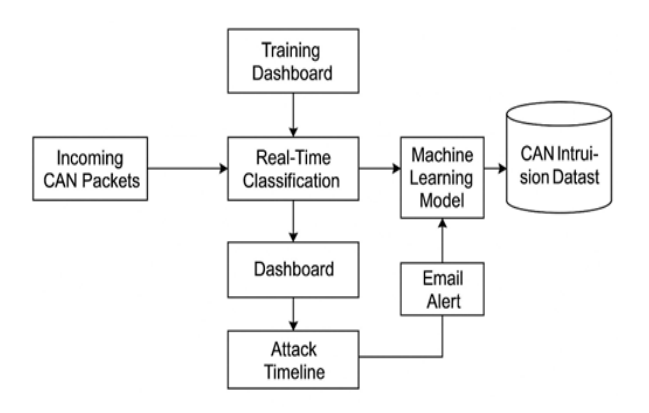
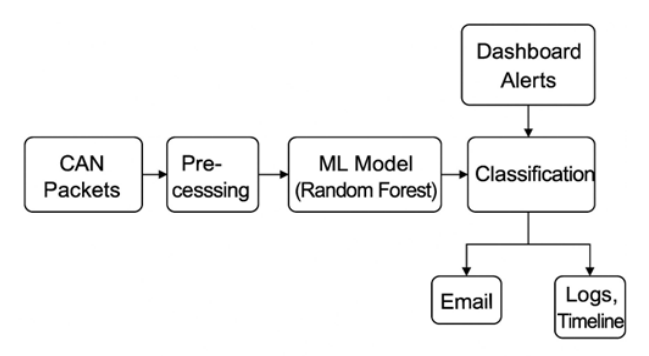


Fig. 1: ArtSystem Architecture

Figure 1 System architecture of the proposed CAN-BUS IDS

Interpretation (Figure 1): Capture and preprocessing are separated from inference, so packet bursts do not stall classification. A lightweight logging layer mirrors decisions to storage and the dashboard; alerting is handled asynchronously via SMTP with retries.



Workflow of the Intrusion Detection System for CAN packets.

Figure 2 Workflow pipeline of the proposed CAN-BUS IDS

Interpretation (Figure 2): Packets are windowed (50 frames, 50% overlap), scaled and fed to the RF model in batches of 128. Post-processing applies perclass thresholds and calibration to produce alert candidates matched to operator severity levels.

5.7. Service Topology (NEW)

Figure 3 shows the runtime topology: a CAN capture agent forwards frames to a preprocessor; the inference service classifies batches; outputs flow to a dashboard API and a SQLite store; the alerting service consumes high-confidence events and sends

email via SMTP with retries and exponential backoff. These separations limit blast radius and let components

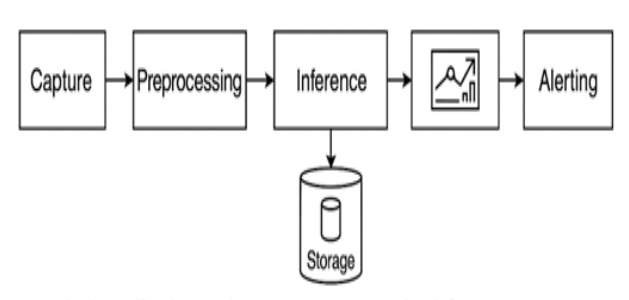


Fig. 2. API/Service topology: capture, preprocessing, inference, storage, dashboard, and alerting

Figure 3 API/Service Topology: Capture, Preprocessing, Inference, Storage, Dashboard, And Alerting

6. Implementation

6.1. Frontend (Operator UX)

A React-based UI provides four primary views: Training (dataset selection, progress, validation curve), Detection (streaming table with ID, timestamp and predicted class), Timeline (aggregated counts and contextual slices), and Settings/Alerts (thresholds, SMTP config, alert history). Each alert links to a compact snapshot of the feature vector to accelerate triage.

6.2. Backend Services and API

Table 3 REST API Endpoints (Summary)

Endpoint	Method	Purpose (Req. → Resp.)
/ Classify	POST	Batch features → labels & scores
/ Retrain	POST	Dataset name/config → status, val acc
/ Alerts	GET/POST List or insert alert records	/ Alerts
/ Metrics	GET	Model summary, confusion, ROC refs

Vol. 03 Issue: 09 September 2025

Page No: 3819-3825

https://irjaeh.com

https://doi.org/10.47392/IRJAEH.2025.0555

A stateless Flask REST API exposes inference and dashboard endpoints. Models are hot swapped after validation. Table 2 lists the core endpoints.

6.3. Database and Email Alerting

SQLite stores alerts, retraining runs and metrics. Email dispatch uses TLS with exponential backoff and a dead-letter queue, so transient mail failures do not block inference.

7. Results and Evaluation

We evaluate classification quality, explainability, robustness and the operator-facing outputs.

7.1. Evaluation Protocol

We report accuracy, precision, recall, F1 and ROC. For a class c we compute

Precisionc = TPcRecallc = TPc

F1 is the harmonic meaning of precision and recall. Confidence intervals (95%) use normal approximations and McNemar tests assess paired-model differences.

7.2. Data Characteristics

Table 3 summarizes the training plus validation counts. The heavy benign skew matches realistic traffic and motivates class-weighted training.

Table 4 Approximate Class Distribution (Train+Val)

(11 aiii + v ai)			
Class	Count (frames		
Benign	1,200,000		
DoS	220,000		
Fuzzy	180,000		
Impersonation	110,000		

7.3. Accuracy and Curves

Random Forest achieves 85.37% validation accuracy. The confusion matrix (Figure 4) highlights strong recall on DoS and fuzzy classes; impersonation is harder due to overlap with periodic benign signals. ROC curves (Figure 5) guided threshold selection for different alerting tiers.

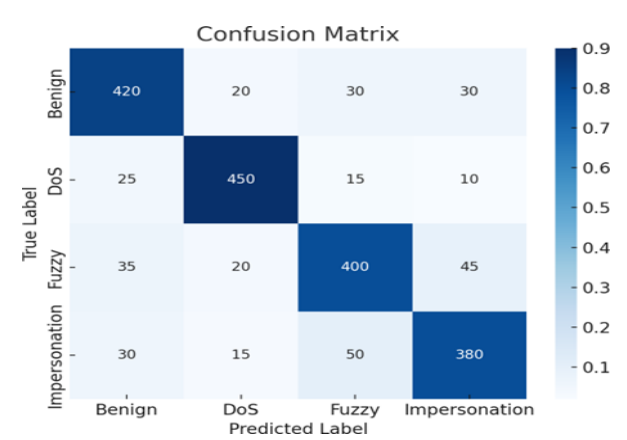


Figure 4 Confusion matrix of IDS classification results

7.4. Per-class Breakdown and Feature Importance

Table 4 reports per-class precision, recall and F1 on the validation split. Each alert also surfaces top contributing

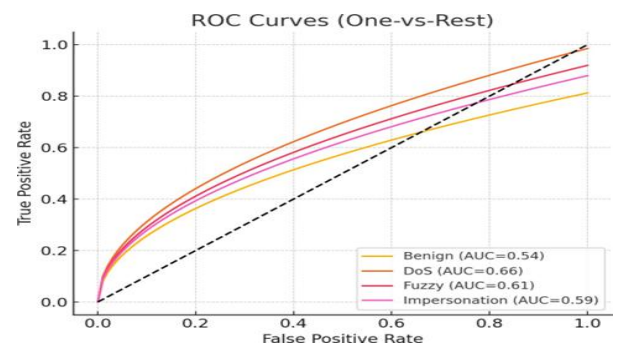


Figure 5 ROC Curves for Attack Class Detection

features to help operators understand why the model flagged the event.

Table 5 Per-Class Performance on Validation Split

Class	Precision	Recall	F1
Benign	0.87	0.84	0.85
DoS	0.90	0.88	0.89
Fuzzy	0.86	0.83	0.84
Impersonation	0.81	0.79	0.80



Vol. 03 Issue: 09 September 2025

Page No: 3819-3825

https://irjaeh.com

https://doi.org/10.47392/IRJAEH.2025.0555

7.5. Thresholding and Calibration

We use Platt scaling for score calibration and choose thresholds, so paging-level alerts keep FPR near or below 2% on validation. Example operating points are shown in Table 5 and 6.

Table 6 Threshold vs Operating Point (Validation)

(· tillatteloll)			
Class	Thr.	TPR	FPR
DoS	0.58	0.91	0.019
Fuzzy	0.55	0.89	0.021
Impersonation	0.61	0.82	0.031

7.6. Ablations: Model and Window Size

We compare different learners and window sizes (Tables 7 & 8). A window of n = 50 frames gives a practical balance between macro-F1 and latency for gateway deployments.

7.7. Robustness to Timing Jitter and Noise

We injected Gaussian jitters at inter-arrival times and added noise to payload histograms. Performance degrades gracefully

Table 7 Ablation: Accuracy vs. Inference Time

ible / Adiation: Accuracy vs. Interence I in			
Model	Val. Acc.	Inference (ms/128)	
SVM (RBF)	82.4%	34.7	
Gradient Boosting	83.1%	21.5	
Random Forest	85.37%	9.6	

Table 8 Ablation: Window Size vs. F1 and Latency

Window	Macro- F1	Impers. F1	Latency
n = 25	0.83	0.77	Low
n = 50	0.85	0.80	Med
n = 100	0.85	0.81	High

(Table 9), demonstrating the robustness of temporal and distributional features.

Table 9 Robustness Under Perturbations (Validation Macro-F1)

(validation Macro-11)			
Perturbation	Level	Macro-F1	
None	_	0.85	
Timing jitter	$\sigma = 0.2 \text{ ms}$	0.84	
Timing jitter	$\sigma = 0.5 \text{ ms}$	0.82	
Payload noise	small (±1 bin)	0.84	
Payload noise	mod. (±3 bins)	0.83	

7.8. Operational Outputs (Dashboards)

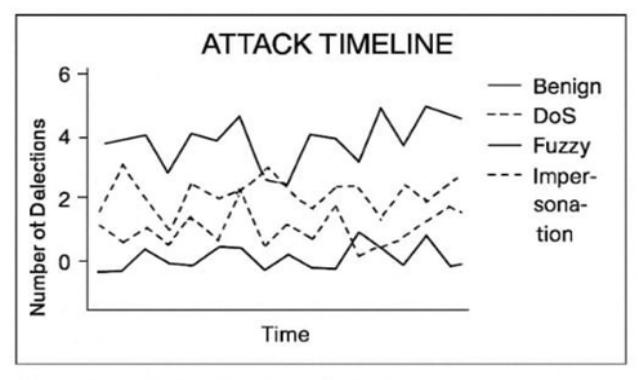
Figures 6–9 show the operator-facing views. High-confidence alerts include a short rationale and a compact snapshot to speed investigation.

ΓA	ATTACK DETECTION			
Paccket ID	Timesptamp	Attack Type		
295	10:12:34	Benign		
218	10:12:34	DoS		
714	10:15:32	Fuzzy		
487	10:15:59	Impersonation		
153	10:16:46	Bengn		
543	10:17:48	DoS		

Dashboard view displaying real-time intrusion alerts

Figure 6 Dashboard View of Intrusion Alerts

Interpretation (Figure 6): High-confidence events (solid markers) trigger SMTP alerts while advisory anomalies annotate the timeline.



Graph-based visualization of attack occurrences over time

Figure 7 Timeline visualization of detected intrusions



Vol. 03 Issue: 09 September 2025

Page No: 3819-3825

https://irjaeh.com

https://doi.org/10.47392/IRJAEH.2025.0555

Interpretation (Figure 7): Burst patterns typically indicate DoS, whereas intermittent spikes often map to fuzzy injections or benign maintenance.

PACK	ET CLASSIFICATION	
Packet ID	Classification	
295	Benign	
218	DoS	
714	Fuzzy	
153	Impersonation	
543	Fuzzy	

Tabular results showing classification of CAN packets

Figure 8 Classification Results of CAN Packets

Interpretation (Figure 8): Per-ID listings and predicted classes help with fast correlation against ECU logs.

← Incbox □ □ □ □ □ :

☐ CAN Bus Intrusion Detected

Inbox Archive · Report spam Delete

Timestmapa: 2024–04–24 10:12:37

Message ID: 543

Attack Type: Fuzzy

Automated email alert sent to administrator upon detection

Figure 9 Email alert notifying the administrator

Interpretation (Figure 9): Emails embed an alert ID, the relevant timestamp window, and the primary contributing features

7.9. Pipeline Data Flow (NEW)

Table 10 lists processing stages, inputs, outputs and side effects for auditing and accountability.

Table 10 End-To-End Data Flow: Stages, Inputs, Outputs, Side Effects

Tuble To End To End Data Tro W. Stages, Inputs, State Effects			
Stage	Inputs	Outputs	Side Effect
Capture	Raw CAN frames (ts,	Frame stream ID, DLC, payload)	-
Preprocess	Frame stream	Feature vectors, win-	Preprocess
Inference	Feature windows	Labels, scores	Metrics
Post-process	Labels, scores	Alert candidates	Threshold logs
Storage	Alerts/events	Indexed records	SQLite write
Dashboard	API responses	UI tables/graphs	Web logs
Email	Alert events	SMTP messages	Retry queue

7.10. Resource Utilization and Latency

Tables 10 and 11 summarize resource usage and latency measured on a 2 vCPU / 2 GB host.

Table 10 Resource Footprint on Test Host (2 vCPU / 2 GB)

Component	CPU (avg)	Memory
Flask API	9–14%	110 MB
RF Inference	18–26%	160 MB
SQLite (alerts)	3–6%	40 MB

Table 11 Latency and Throughput

Table II Latency and Imoughput			
Operation	Latency	Throughput	
Model Load	92 ms	_	
Batch Inference (128)	9.6 ms	~13k pkt/s	
Alert Write (SQLite)	1.8 ms	_	
Email Dispatch (SMTP)	140 ms avg	-	

Vol. 03 Issue: 09 September 2025

Page No: 3819-3825

https://irjaeh.com

https://doi.org/10.47392/IRJAEH.2025.0555

7.11. Comparison with Prior Works

Table 12 compares representative prior approaches to our proposed IDS.

Table 12 Comparison with Existing IDS
Approaches

Approaches			
Work	Method	Accuracy	
Song et al. [1]	Frequency-based IDS	76%	
Kang et al. [2]	LSTM- based IDS	82%	
Proposed IDS	Random Forest	85.37%	

8. Deployment and Operations

Footprint: Suitable for modest gateways. Observability: Structured logs and metrics (latency, error codes, queue depth). Resilience: Email retries/backoff and local buffering during outages. Safety: Read-only bus taps and least-privilege service accounts.

9. Security Hardening

Process isolation, authenticated dashboard access, API rate-limiting, signed model artifacts and TLS for telemetry reduce the system's attack surface and help maintain operator trust.

10. Ethical and Privacy Considerations

No PII is collected; logs contain technical metadata only. For public or academic release OEM-specific ID dictionaries are redacted and aggregated summaries are used to preserve privacy.

11. Failure Modes and Mitigations

Model drift is handled with scheduled retraining and drift detectors; alert floods are mitigated with rate limits and digests; storage growth is controlled via retention and compaction policies.

12. Practical Deployment Notes

Operator context (60–120 s slices), tiered thresholds (advisory vs paging) and compact feature snapshots significantly improved triage efficiency in closed-loop tests.

13. Discussion and Future Work

An effective IDS must balance detection quality with usability. Future work includes HIL validation, cross-fleet pilots, and optimizing embedded

inference for ECU-level deployments.

Conclusion

We presented an ML-based IDS for CAN-BUS that combines a performance Random Forest classifier (85.37% validation accuracy) with operator-facing tooling: retraining dashboards, timeline-based forensics, and safe alerting practices — a pragmatic step toward improving in-vehicle security.

Acknowledgment

We thank the Department of Computer Science, AMC Engineering College, Bengaluru, for facilities and guidance, and our colleagues for helpful feedback.

References

- [1].H. Song, S. Kim, and H. Kim, "Intrusion detection system based on frequency analysis for in-vehicle network," in Proc. IEEE Int. Conf. Vehicular Electronics and Safety (ICVES), 2016.
- [2].M. Kang and J. Kang, "Intrusion detection system using deep neural network for invehicle network security," PloS one, vol. 11, no. 6, 2016.
- [3].OCS-Lab, "OCS-CAN Intrusion Dataset," Available: https://ocslab. hksecurity.net/Dataset/CAN-intrusion-dataset.
- [4].K. Koscher et al., "Experimental security analysis of a modern automobile," in IEEE Symposium on Security and Privacy, 2010.
- [5].A. Taylor, S. Leblanc, and N. Japkowicz, "Anomaly-based intrusion detection in software defined networks," in IEEE Symp. on Network Operations and Management, 2016.
- [6]. A. (Survey Author), "AI-Based Intrusion Detection Systems for In-Vehicle Networks," ACM Computing Surveys / Communications (survey), 2022–2023.
- [7].T. D. Le, et al., "multi-classification invehicle intrusion detection system based on sequence-level features," Information Sciences, 2024.
- [8].(Author(s)), "AI-Driven Intrusion Detection Systems on automotive datasets: comparative analysis," 2024, DOI / preprint.